



Hydrogeological processes and geological settings over Europe controlling dissolved geogenic and anthropogenic elements in groundwater of relevance to human health and the status of dependent ecosystem

## Deliverable D4.2

**Degradation and mineralisation of selected contaminants in European GW-SW transition zones**

Authors and affiliation:  
**Tina B Bech, GEUS**

**Jens Aamand, GEUS**

**Jennifer Hellal, BRGM**

E-mail of lead author:  
**tib@geus.dk**

Version: 26-10-2021

This report is part of a project that has received funding by the European Union's Horizon 2020 research and innovation programme under grant agreement number 731166.



Deliverable Data		
<b>Deliverable number</b>	D4.2	
<b>Dissemination level</b>	Public	
<b>Deliverable name</b>	Degradation and mineralisation of selected contaminants in European GW-SW transition zones as input to task 4.3	
<b>Work package</b>	WP4	
<b>Lead WP/Deliverable beneficiary</b>	Jens Aamand, GEUS	
Deliverable status		
<b>Submitted (Author(s))</b>	27/10/2021	Tina B Bech, Jennifer Hellal
<b>Verified (WP leader)</b>	27/10/2021	Jens Aamand
<b>Approved (Coordinator)</b>	27/10/2021	Laurance Gourcy





## TABLE OF CONTENTS

1	INTRODUCTION .....	2
2	SITE OVERVIEW .....	4
2.1	River Crieu.....	4
2.2	Risby stream .....	5
2.3	Holtum Stream.....	6
2.4	Planned work at each site.....	8
2.4.1	Selected organic contaminants.....	9
3	RESULTS.....	10
3.1	Mineralization and degradation .....	10
3.1.1	Mineralization .....	10
3.1.2	Degradation .....	10
3.1.3	River Crieu.....	10
3.1.4	Risby stream.....	13
3.1.5	Holtum stream .....	15
3.2	Degradation rates (DT <sub>50</sub> ).....	21
3.2.1	River Crieu.....	21
3.2.2	Risby stream.....	22
3.2.3	Holtum stream .....	23
4	CONCLUSION .....	24
5	REFERENCES.....	26



## 1 INTRODUCTION

It is well known that rivers facilitate drainage pathways for watersheds. In addition, it also provides several different ecosystem services, including fresh drinking water, renewable energy production, and environments for wildlife and human recreation.

However, the hydrological processes are more complex than the before mentioned drainage pathway because an exchange of water occurs within the riverbed sediments and between the surface water and the underlying groundwater. These vertical and lateral exchanges with more slowly moving waters in the sediments surrounding the river increase the residence time of dissolved and suspended particles and pollutants and thus increase the likelihood of biological and geochemical processes (Boano et al., 2014). Therefore, the river corridor, and not just the river itself, plays an essential role in ecohydrology, including the transformation of organic pollutants (Lewandowski et al., 2019).

The sediment within the “hyporheic zone” (HZ) is a unique habitat located at the interface of surface water and groundwater within river corridors. While the term hyporheic zone is sometimes used as a synonym for the streambed, it is more accurately the zone in which surface water and groundwater mix. The HZ is an interfacial zone important to many key stream processes and organisms. Because of the large surface area of sediment grains within the streambed and the high activity of microbes living in the HZ, it plays a vital role as a reactive zone, transforming pollutants and natural solutes and providing a habitat for benthic communities. Hence, the hyporheic zone has been termed the ‘river’s liver’ (Fischer et al. 2005).

Transformation of pollutants in the hyporheic zone is influenced by many different processes, including hydrological (e.g., transport of water and solutes), chemical (e.g., sorption, chemical reactions), and biological processes (e.g., microbial activity, bioturbation):

- **Hydrology.** The water flow velocity and direction are dependent on the hydraulic conductivity of the sediment and the height difference between the hydraulic heads, i.e., the height of the aquifer and the level of the river water. Based on these geological and hydrological conditions, distinct sections of gaining or losing conditions are present along a river. Due to seasonal water levels, the flow direction can also shift from gaining to losing and vice versa.
- **Chemical.** The primary attenuation process in the HZ is sorption of pollutants to either organic matter, clay or various oxides present in the sediment or biodegradation by bacteria and fungi (Smith, 2005). The degree of sorption is mainly described by the sediment/water partitioning constant  $K_d$  and can influence the flux of pollutants through a sediment layer. The degree of sorption to sediments will influence the residence time and potentially biodegradation in the hyporheic sediment.
- **Biology.** The flow between surface and groundwater follows complex dynamics (Rutherford and Hynes, 1987), in which upwelling and downwelling zones occur alternately (White, 1990). The ecology is strongly influenced by predominant water flow directions, where oligotrophic organisms are in favor when upwelling nutrient-poor



groundwater is inflowing. On the opposite, there is generally high biological activity under downwelling conditions due to high nutrient input from surface water (Peralta-Maraver et al., 2018). Highly variable flow conditions may change sediment conditions even at the centimeter scale, both spatially and temporary (Boano et al., 2014; Wondzell, 2011).

The interaction of these processes in the hyporheic zone creates a diverse array of ecosystem services, including transforming organic pollutants and removing nutrients (Krause et al., 2009; Lewandowski et al., 2011).

Many studies have described nitrogen, phosphorus and organic carbon attenuation in the hyporheic zone (Aubeneau et al., 2015; Harvey et al., 2013; Stegen et al., 2016). While the transformation of these common substrates is widespread (Battin et al., 2016), the degradation of organic contaminants, such as pesticides and pharmaceuticals, may be more complex, involving combined metabolic activities of the hyporheic zone microbial community (Krause et al., 2009; Peralta-Maraver et al., 2018). Microbial degradation of pollutants is impacted by several parameters, including hyporheic exchange flows, subsurface residence time, temperature, redox conditions, organic carbon content and the microbial community structure (Hebig et al., 2017; Lewandowski et al., 2019; Munz et al., 2019). Posselt et al. (2020) found that hyporheic systems holding a higher microbial species richness and diversity were more efficient at attenuating a more significant number of pharmaceuticals. However, the literature describing the fate and removal rates of pesticides in hyporheic sediments is sparse (Köhler and Triebkorn, 2013; Lewandowski et al., 2011).

WP4 focuses on linking aquifer microbial ecology to contaminant transformation processes in the hyporheic zone within the HOVER project. The main aim has been to determine the potential for degradation of organic pollutants in the hyporheic zone and link this to the microbial community composition. Where D4.2 focuses on degradation results, D4.3 focuses on the microbial community composition.



## 2 SITE OVERVIEW

The main objective of WP4 is to increase our understanding of how groundwater ecology and microbial diversity determine contaminant-transforming processes at European groundwater-surface water (GW-SW) transition zones (hyporheic zones). To do this, three field sites were selected, two in Denmark and one in France. In common for the three sites is a solid knowledge of hydraulic heads and conductivities and, to some extent, knowledge of existing pollutants in the areas. The site in France and the Holtum stream in Denmark are impacted by agriculture, whereas the Risby site in Denmark is located near a landfill. Both situations are relevant to increase our knowledge on the degradation of contaminants in the hyporheic zone within streams. Detailed information on the French and the landfill impacted Danish site can be found in Deliverable D4.1. This deliverable also contains information on a Latvian site that was abandoned due to travel restrictions resulting from the covid 19 pandemic. Instead, another Danish location (The Holtum stream) was selected for the research. Below, a short description of each of the three sites is given.

### 2.1 River Crieu

The study site in France is located in the alluvial plain of the Ariège River Basin, on the Crieu River (Figure 1). The alluvium was deposited in five distinct terraces of somewhat similar composition. The aquifer is unconfined, and the unsaturated zone is generally <10m thick. The alluvial plain is mostly cultivated farmland, mainly corn. This basin has been studied previously, which enabled us to choose locations along the river.

The main pesticides found in the groundwater along this river basin are (S-)metolachlor and, to a lesser extent, atrazine that was withdrawn from the market in 2003. Besides pesticides, also metabolites of pesticides (notably chloroacetanilides) have been found previously in high amounts (Amalric et al., 2013).

The study points for groundwater identified for the HOVER project are located in the middle and downstream stretches of the Crieu River. The infiltration of river water characterizes the first, Villeneuve du Paréage (Pz Vill), into the aquifer below. In contrast, the downstream site, Saverdun (Pz Sav), is characterized by an upwelling of groundwater towards the river (Figure 1). Samples for stream water and sediment analyses (chemistry, degradation potential and diversity) were collected from 6 points along the river section (CP3, CP4, CP5, CP6, CP6b and CP7) (Figure 1).

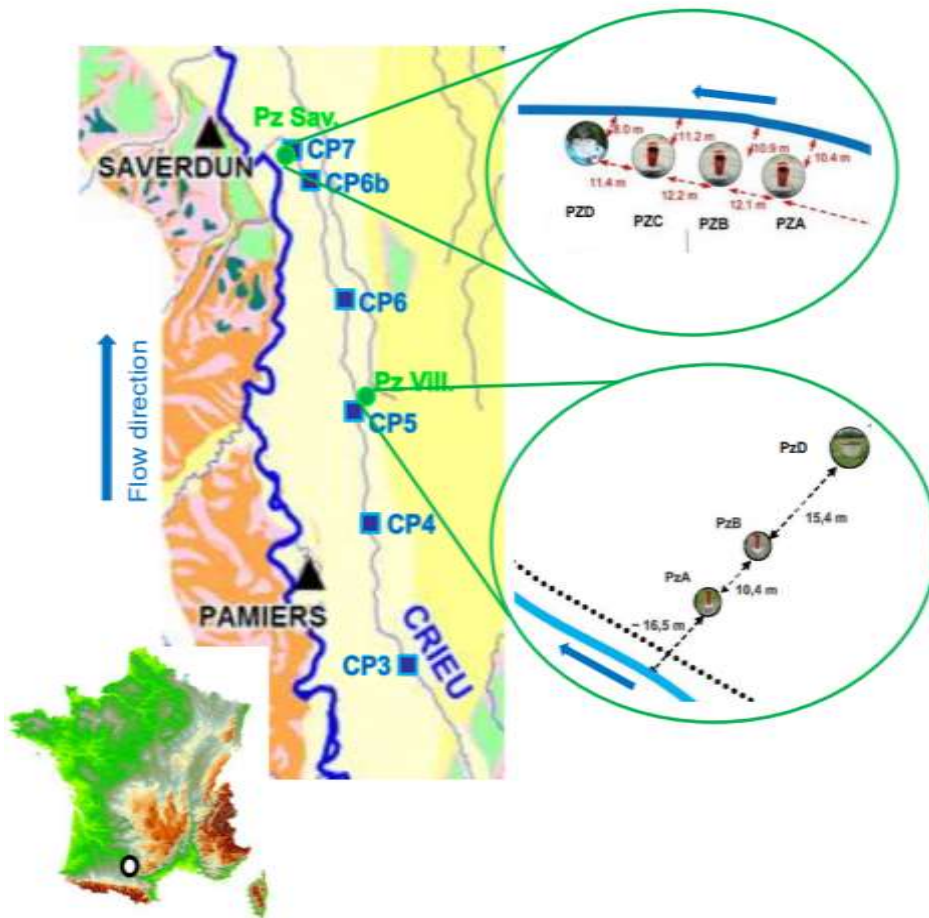


Figure 1. Localization of the Crieu River and the sampling spots identified for HOVER.

## 2.2 Risby stream

The Risby Landfill is located west of Copenhagen and was actively used from 1959 to 1981. It covers an area of 6.5 ha and contains a total of 500,000 m<sup>3</sup> of waste. There are no liners or leachate collection systems installed at the landfill. Although no detailed records exist, it contains a mixture of municipal waste, demolition waste, fly ashes, and some chemical waste. The potential for pesticide degradation in the hyporheic zone of the Risby stream has been studied previously where it was shown that locations with the highest mass discharge of pesticide had the highest degradation potentials (Batioğlu-Pazarbaşı et al., 2013). The groundwater flow direction from the landfill is towards the stream with varying water discharge volumes, as seen in Figure 2.

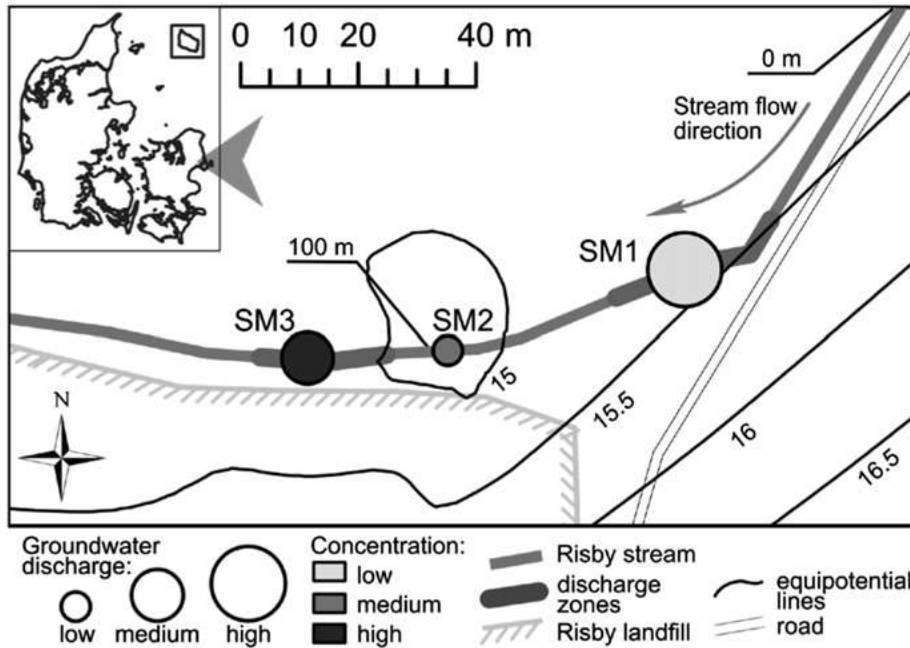


Figure 2. Sampling locations of the Risby Landfill and groundwater discharge zones. Groundwater was collected from the three seepage meters (SM1, SM2, SM3), and streambed sediments were collected in the vicinity of the SM. Sampled discharge zones have different pesticide mass discharges due to variations in the groundwater discharge and pesticide concentration (Batioğlu-Pazarbaşı et al., 2013). SM4 was sampled 100 m upstream from SM1.

### 2.3 Holtum Stream

The study was conducted in the groundwater-gaining lowland Holtum stream, located in the Skjern river catchment in Jutland, western Denmark (Fig. 1a). This glacial floodplain valley is characterized by thick sediment deposits of sand and silt deposited during the latest Weichsel glacial period (Houmark-Nielsen, 1989), and with podzols being the dominating soil layers.

Between stations 1 and 4, the stream flows from east to west with a mean gradient of 1 ‰. Beyond a riparian zone of approximately 5 m, station 1 is surrounded by agricultural fields, whereas the near-stream areas at stations 2, 3 and 4 are wetlands. The mean annual discharge, the topographical catchment and land use of sub-catchments to each station are summarized in Table 1.

The main objective of the Holtum sampling was to compare the transformation of organic pollutants at station 1 (agricultural) and station 4 (natural) in the upper and lower sediment from the hyporheic zone and compare these transformations to the abundance and diversity of the bacterial community (Figure 3).



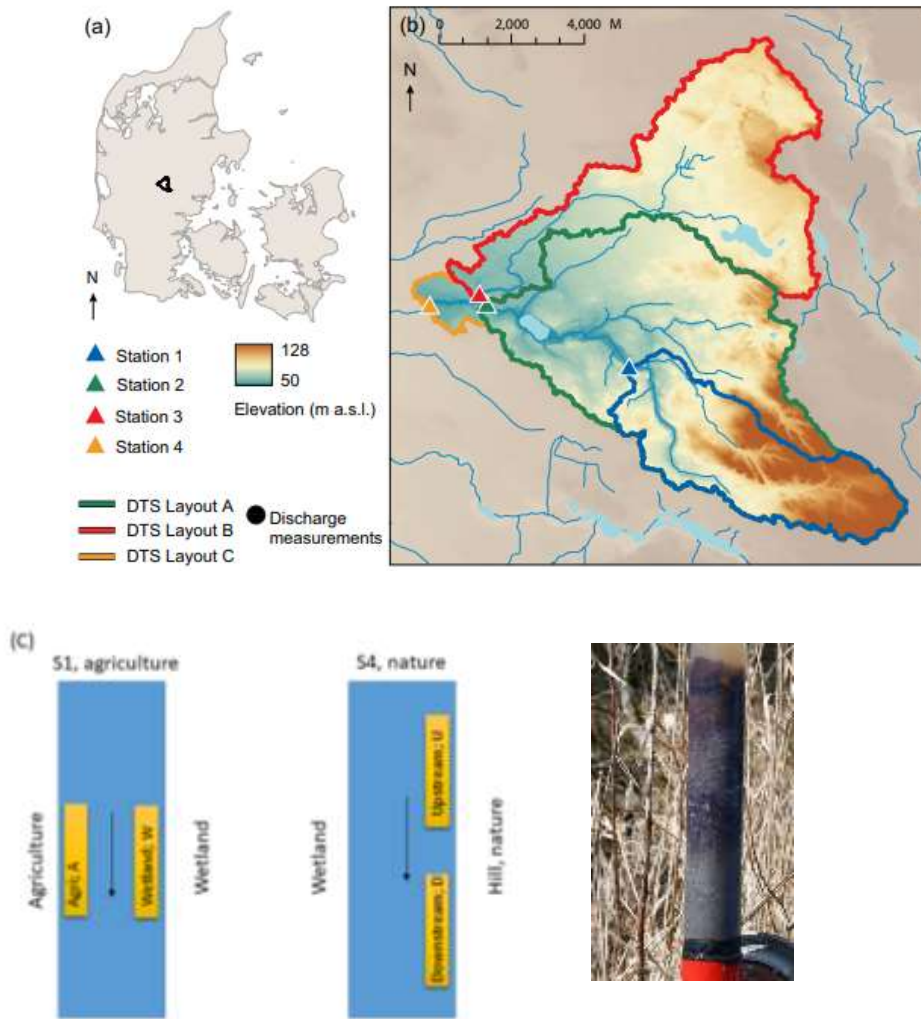


Figure 3. Overview of the different stations along the Holtum stream (A and B) (Poulsen et al., 2015). In the present study, only stations 1 and 4 were included (C), where station 1 (S1) is agriculturally impacted, and station 4 (S4) is surrounded by wetlands (C). The soil columns show the two investigated horizons from the four sampling locations (yellow squares in C), giving upper organic-rich sediment and a lower sandy sediment (photo).



Table 1. Catchment characteristics and land use for each sub-catchment, with mean annual discharge, catchment size, specific discharge, distance from the source and land use (Poulsen et al., 2015)

	<i>Mean annual discharge</i>	<i>Catchment size</i>	<i>Distance from the source</i>	<i>Urban</i>	<i>Agriculture</i>	<i>Forest</i>
	m <sup>3</sup> s <sup>-1</sup>	km <sup>2</sup>	m	%		
Station 1	0.17	26	6.6	27	51	20
Station 2	0.8	70	12.7	21	56	22
Station 3	0.28	42	11.6	16	41	41
Station 4	1.2	114	14.7	13	53	34

## 2.4 Planned work at each site

Figure 4 provides an overview of the planned work at each site, including the effect of organic carbon, redox conditions, pH, and temperature on contaminant degradation and mineralization. Complete mineralization was determined from microcosm studies with sediments and water using <sup>14</sup>C labeled pollutants. Degradation rates (DT<sub>50</sub>) were determined from microcosm studies with river sediments.

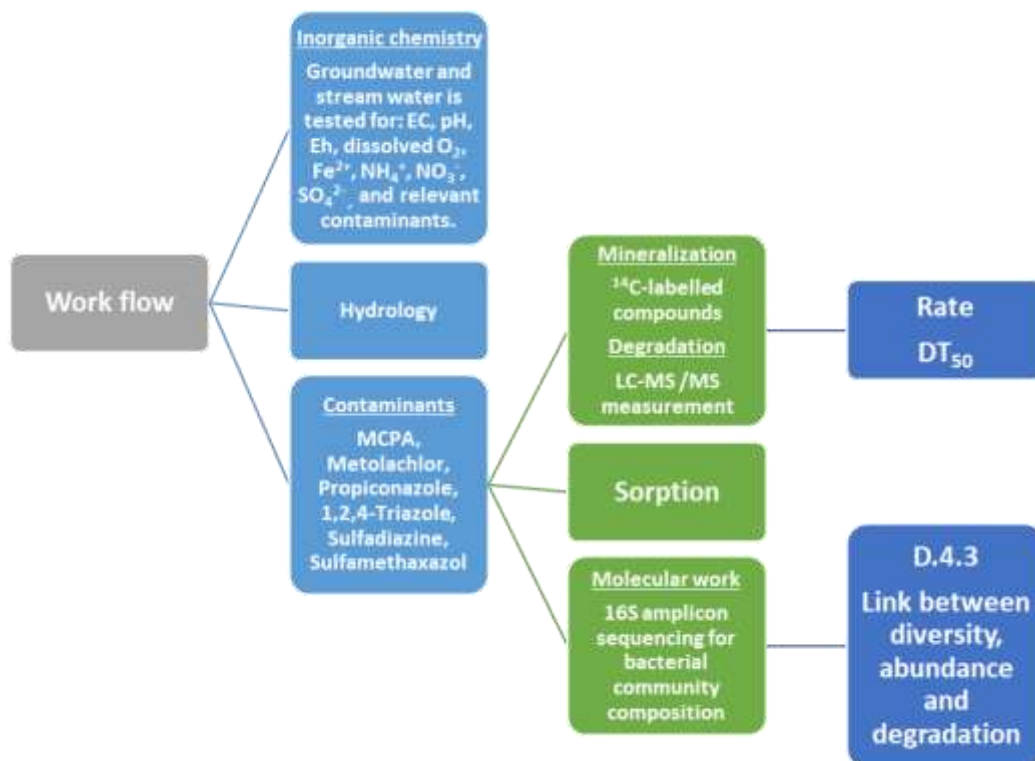


Figure 4. Overview of the planned work at each of the three sites. The link between diversity, abundance and degradation will be presented in deliverable D4.3, which will be based on the given data in this deliverable D4.2.



### 2.4.1 Selected organic contaminants

Two herbicides (MCPA, metolachlor), one fungicide (propiconazole), and two representatives of the widely used class of sulfonamide antibiotics, namely sulfamethoxazole and sulfadiazine, were selected (see Table 2).

Table 2. Physical-chemical properties and main biodegradation patterns.

<b>Compound</b>	<b>M</b>	<b>Water solubility</b>	<b>K<sub>d</sub></b>	<b>pKa</b>	<b>Aerobic degradation (DT<sub>50</sub>)</b>	<b>Type</b>
	(g/mol)	(mg/L)	(L/kg)		days	
MCPA	200.62	630	0.7 – 1	3.09	7 – 41	Herbicide
Metolachlor	283.79	530	1; 4 – 8	-	14 – 169	Herbicide
Propiconazole	342.2	100	4 – 29		25 - 315	Fungicide
Sulfadiazine	250.28	77	1.2	6.36		Antibiotic
Sulfamethoxazole	253.28	610	1.2	5.7		Antibiotic



## 3 RESULTS

### 3.1 Mineralization and degradation

#### 3.1.1 Mineralization

Mineralization of metolachlor, MCPA, propiconazole, and 1, 2, 4- triazole were determined in triplicate microcosms with sediments from each of the three locations. Experiments were set up in glass vials with 2.5 g (wet weight) sieved and homogenized sediment and 0.5 ml river water for full saturation.  $^{14}\text{C}$ -labeled metolachlor, MCPA, propiconazole, and 1, 2, 4-triazole were prepared and spiked to an initial concentration of  $10 \mu\text{g kg}^{-1}$  sediment (wet weight) and approximately 10.000 DPM. A test tube containing 1 ml of 1 M NaOH was placed in the flask to capture  $^{14}\text{CO}_2$  formed by mineralization. The flasks were closed airtight and kept in the dark at  $10^\circ\text{C}$ . The NaOH solution was replaced and analyzed between day 4 and day 150 after the initial setup. The NaOH solution was added to 10 mL Optiphase HiSafe 2 scintillation liquid (Wallac, Finland), and the  $^{14}\text{CO}_2$  content was determined using a Perkin Elmer Tri-Carb 2810 TR liquid scintillation counter (LSC).

#### 3.1.2 Degradation

Microcosms were prepared with 2.5 g (wet weight) sediment and 0.5 ml river water to ensure saturation. Samples were spiked with a mix of MCPA, metolachlor and propiconazole to a concentration of  $12 \mu\text{g/kg}$ . Thrice autoclaved samples ( $121^\circ\text{C}$ , 21 minutes) were used as abiotic controls. All samples were subsequently incubated at  $10^\circ\text{C}$  in the dark.

Analysis of target compounds, including their metabolites, was performed by ultrahigh-pressure liquid chromatography coupled with tandem mass spectrometry carried out on a Waters Acquity UPLC coupled to a Waters Xevo TQ-S tandem quadrupole with electron spray ionization. A Waters Acquity UPLC HSS C18 column with  $1.9 \mu\text{m}$  particle size, 2.1 mm inner diameter and a length of 100 mm was operated at a temperature of  $26^\circ\text{C}$ . The flow rate was set to 0.3 ml/min, and an injection volume of  $80 \mu\text{l}$  was used. Mobile phases used were Milli-Q water with 0.1 % formic acid (phase A) and acetonitrile (phase B). Gradient elution was used starting at 10 % phase B held constant for 0.5 minutes. Mobile phase B was increased to 40 % 6 minutes after injection, ramped up to 95 % B at 8.1 minutes after injection and held constant for 0.9 minutes.

#### 3.1.3 River Crieu

In the River Crieu sediments, we measured the mineralization and degradation of the following compounds: MCPA (Figure 5), metolachlor (Figure 6) and propiconazole (Figure 7).

Mineralization curves, showing accumulated amounts of  $^{14}\text{CO}_2$  released from mineralization of  $^{14}\text{C}$ -MCPA over time, revealed 47 % mineralization after 116 days (Figure 5A). The mineralization pattern revealed a rapid mineralization rate, followed by slow mineralization, where the maximum mineralization potential was reached after approximately 50 days. MCPA degradation was fast and fitted the single-first-order kinetics in all samples. After day 60, the majority of MCPA has been degraded (Figure 5B).

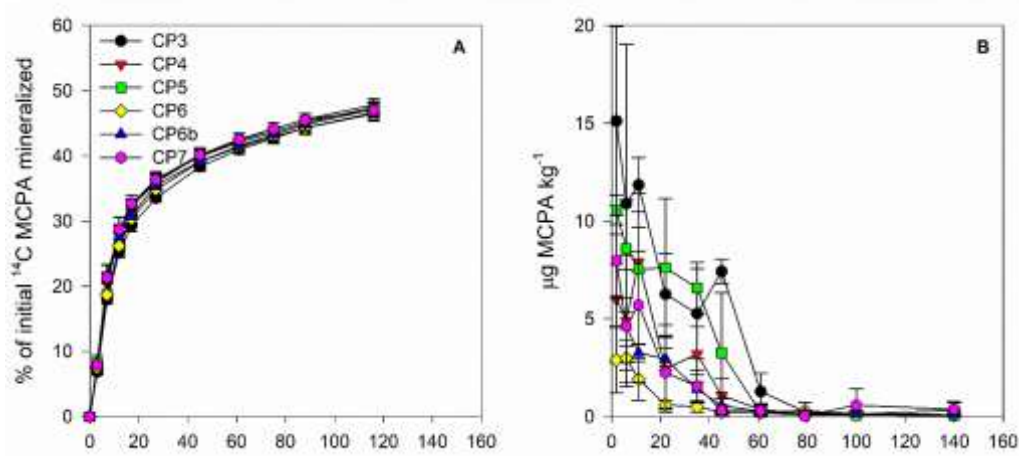


Figure 5. Mineralization of MCPA (A) and degradation of MCPA (B) in Crieu river sediments. Standard deviations are based on triplicate biological measurement.

Mineralization curves showing accumulated amounts of  $^{14}\text{CO}_2$  released from mineralization of  $^{14}\text{C}$ -metolachlor over time revealed from 7 to 16 % mineralization after 146 days (Figure 6A). Concomitantly to mineralization, degradation of metolachlor (MTC) occurred (Figure 6B). Degradation of MTC was observed in all sediments, and at day 146, less than  $2 \mu\text{g MTC kg}^{-1}$  sediment was detected. The degradation of MTC was followed by the accumulation of the degradation products, metolachlor oxalic acid (MOA) and metolachlor ethansulfonic acid (MESA) in concentrations from  $0.5$  to  $1.0 \mu\text{g MOA/MESA kg}^{-1}$  sediment (Figure 6C and 6D). In sterile controls, no degradation was observed, indicating biodegradation as the primary pathway for metolachlor degradation in these samples.

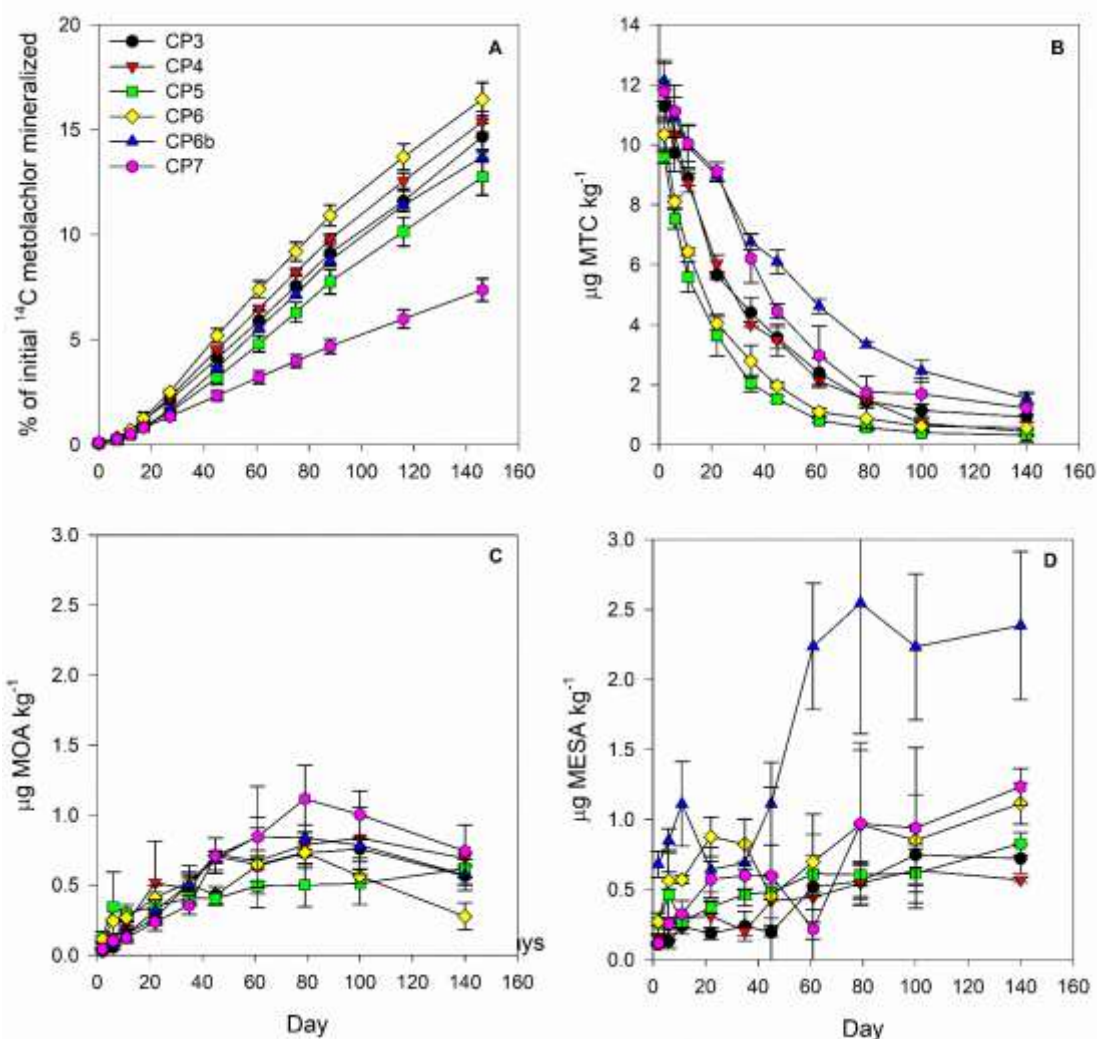


Figure 6. Mineralization of metolachlor (A), degradation of metolachlor (B), MOA (C), MESA (D) in Crieu river samples. Standard deviations are based on triplicate measurement.

Mineralization curves showing accumulated amounts of <sup>14</sup>CO<sub>2</sub> released from mineralization of either propiconazole <sup>14</sup>C-labelled at the benzene or triazole ring are shown in figure 7A and 7B, respectively. When propiconazole was labeled in the benzene ring, there was 17–35 % mineralized depending on the sediments, whereas no mineralization was observed from the triazole labeled propiconazole. For the transformation product, 1,2,4-triazole mineralization ranged from 35–48 %. Degradation of propiconazole was observed in all sediments, and at day 146, between 4–6 µg propiconazole kg<sup>-1</sup> sediment was detected (7D).

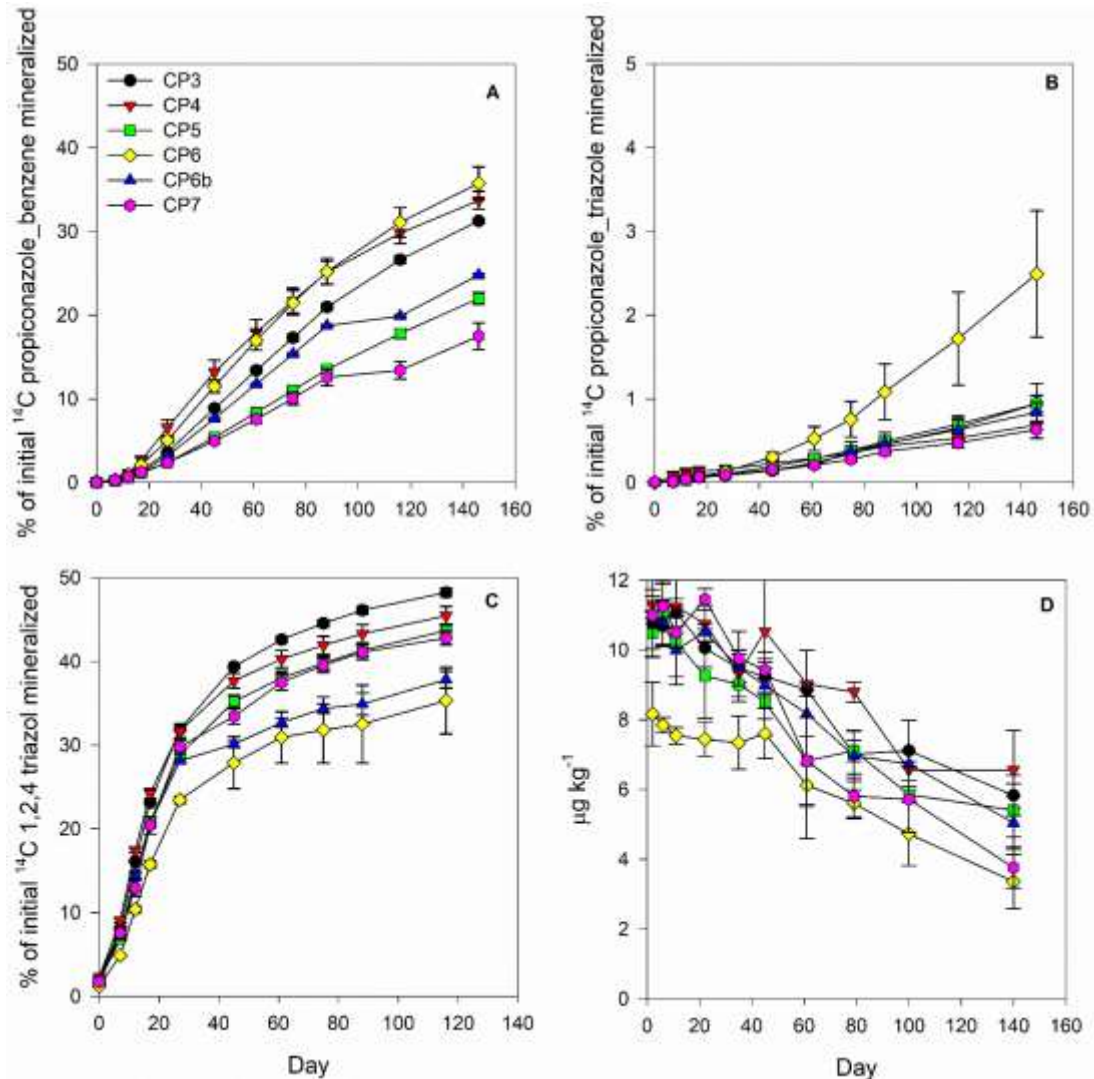


Figure 7. Mineralization of propiconazole  $^{14}\text{C}$  labeled in the benzene ring (A), mineralization of propiconazole  $^{14}\text{C}$  labeled in the triazole ring (B), mineralization of 1,2,4-triazole (C) and degradation of propiconazole (D) in Crieu river sediments. Standard deviations are based on triplicate measurement.

### 3.1.4 Risby stream

Aerobic mineralization experiments in the sediment layer revealed limited biological activity. MCPA mineralization was observed from the beginning of the experiment without an apparent lag phase (Erreur ! Source du renvoi introuvable.8). A plateau was observed at the end of the experiment (130 days) with a maximum of 16 % of the added compound mineralized at site SM3. The mineralization was most rapid at SM3 and SM4, where 10 % was mineralization after 12 days. Slower mineralization was seen in SM1 and SM2, where 10% mineralization was achieved, after 26 days and 50 days, respectively. The control microcosm showed no  $^{14}\text{CO}_2$  evolution, excluding abiotic mineralization. Mineralization was also observed for 1,2,4-triazole, a metabolite of propiconazole degradation (8). The highest percentage of evolved  $^{14}\text{CO}_2$  was observed in SM3 and SM4. Overall, the mineralization of 1,2,4-triazole was slower than MCPA, surpassing 10 %



levels at the end of the experiment after 130 days in SM2, SM3 and SM4. Again, no  $^{14}\text{CO}_2$  was measured in the abiotic control, excluding abiotic mineralization of 1,2,4-triazole. No mineralization was observed in microcosms added  $^{14}\text{C}$ -labelled propiconazole (labeled either on the benzene or the triazole ring), sulfadiazine or metolachlor.

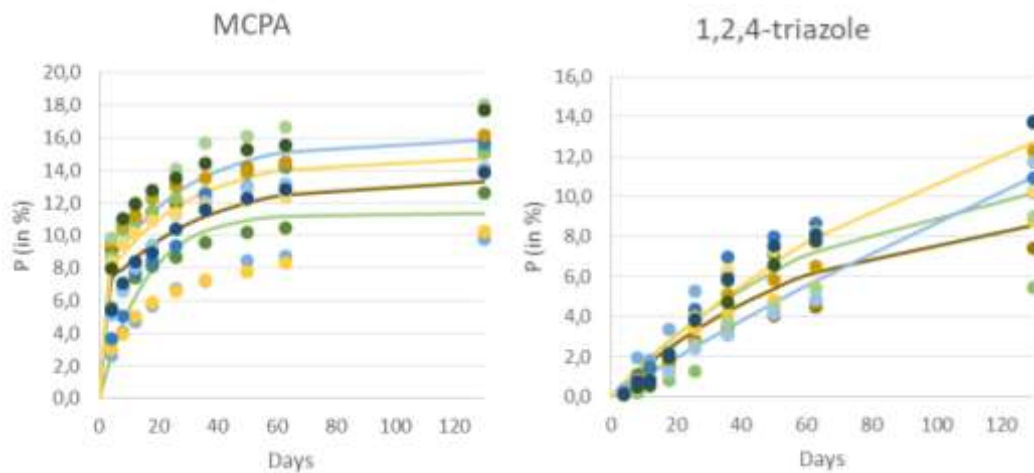


Figure 8. Mineralization of MCPA and 1,2,4-triazole. Lines represent kinetic model fit; symbols replicate measurements. SM1, SM2, SM3, SM4

Overall, mineralization experiments only showed limited activity at the Risby site. MCPA has been shown to be readily biodegradable with 45 to 70 % of the added compound mineralized to  $\text{CO}_2$  (Bælum et al., 2012). However, maximum mineralization reached only 16 % in this experiment (Figure 8). The second compound undergoing mineralization was 1,2,4-triazole reaching 8.5 to 12.3 % of initial added compound converted to  $\text{CO}_2$ . Mineralization at site SM1, receiving the highest groundwater discharge from the landfill site, appeared to be slowest for 1,2,4-triazole. This could be a first indicator of an influence of polluted groundwater discharge on mineralization rates. However, differences between sample sites are small and no clear conclusion about differences from groundwater discharge rates can be drawn. Furthermore, MCPA mineralization showed a different pattern amongst the different sample sites, preventing a conclusion about a clear influence of discharge flow rates on overall mineralization potential.

Contrary to metolachlor mineralization, degradation was observed, as only 8 to 13 % of the added metolachlor was left after 100 days, indicating a partial degradation of metolachlor (Figure 9). Only metolachlor oxalic acid, one of the two major degradation products, accumulated in the degradation experiment with maximum concentrations below  $0.5 \mu\text{g}/\text{kg}$ . This would imply incomplete transformation of metolachlor with the formation of unknown degradation products. On the other hand, fast degradation of the metolachlor oxalic acid and ethansulfonic acid (MOA and MESA) metabolites could also explain their absence in the analysis. No degradation was observed in the sterile controls, indicating biodegradation as the primary pathway for metolachlor dissipation.

Degradation of MCPA appeared to be relatively fast with computed  $\text{DT}_{50}$  values between 6 and 14 days (Erreur ! Source du renvoi introuvable.4).



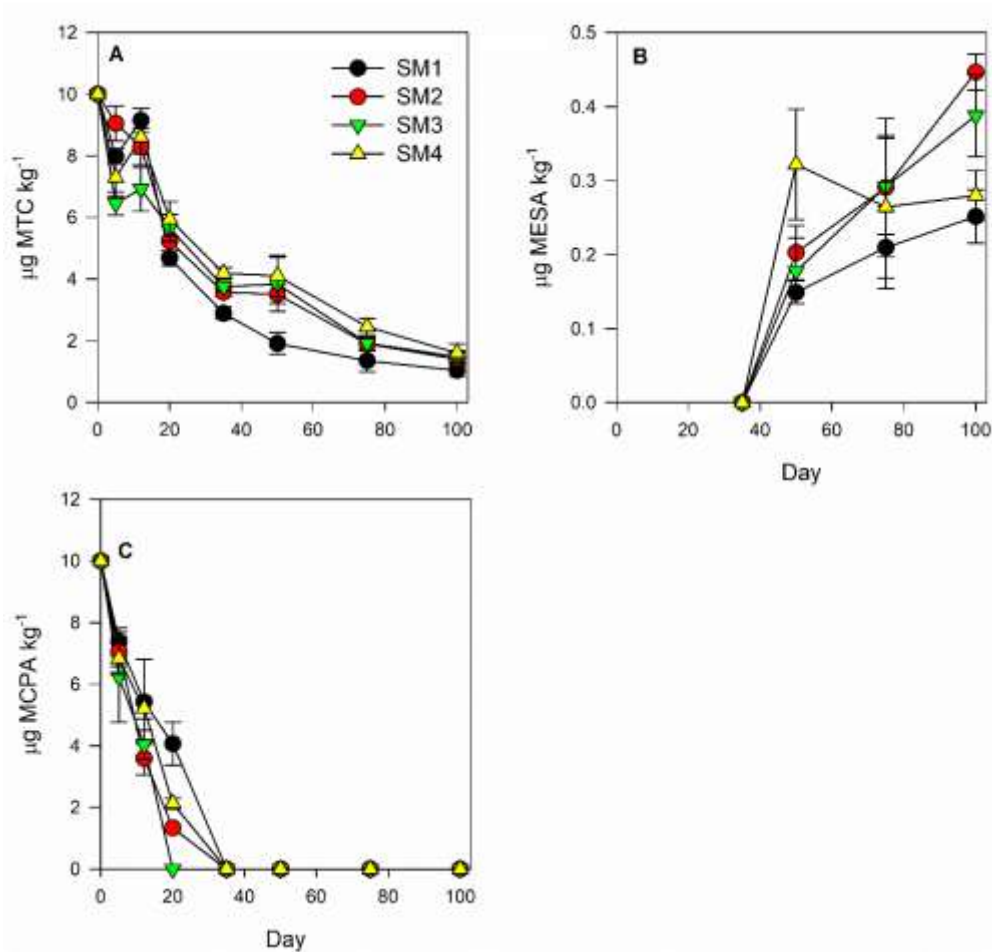


Figure 9. Degradation of metolachlor (A), accumulation of MESA (B) and degradation of MCPA (C) in Risby sediments.

### 3.1.5 Holtum stream

In Holtum stream sediments, we observed mineralization of MCPA, metolachlor, bentazone and 1,2,4-triazole (Figure 10 and 11). In general, there was low mineralization at stations 1 and 4, except for MCPA, which reached about 30 %. However, a large standard deviation and low purity of the labeled MCPA means that these data should be analyzed with precaution.

For both bentazon and metolachlor, it appears that from station 1, there is a higher mineralization potential in the lower B horizon than the A horizon and from both horizons at station 4. For 1,2,4-triazole there were no clear trends and in general approximately 4-10 % was mineralized. The mean annual groundwater discharge is approximately 10 timer higher at station 4, and could be a potential reason behind lack of mineralization in the B horizon at station 4 – importantly, this is very speculative due to the low number of data. During the sampling campaign we measured the upwelling water velocity, and here only S4 upstream differed from the other three locations with an inflow that was ~50 times faster. Again this does not seem to be an important parameter for mineralization.

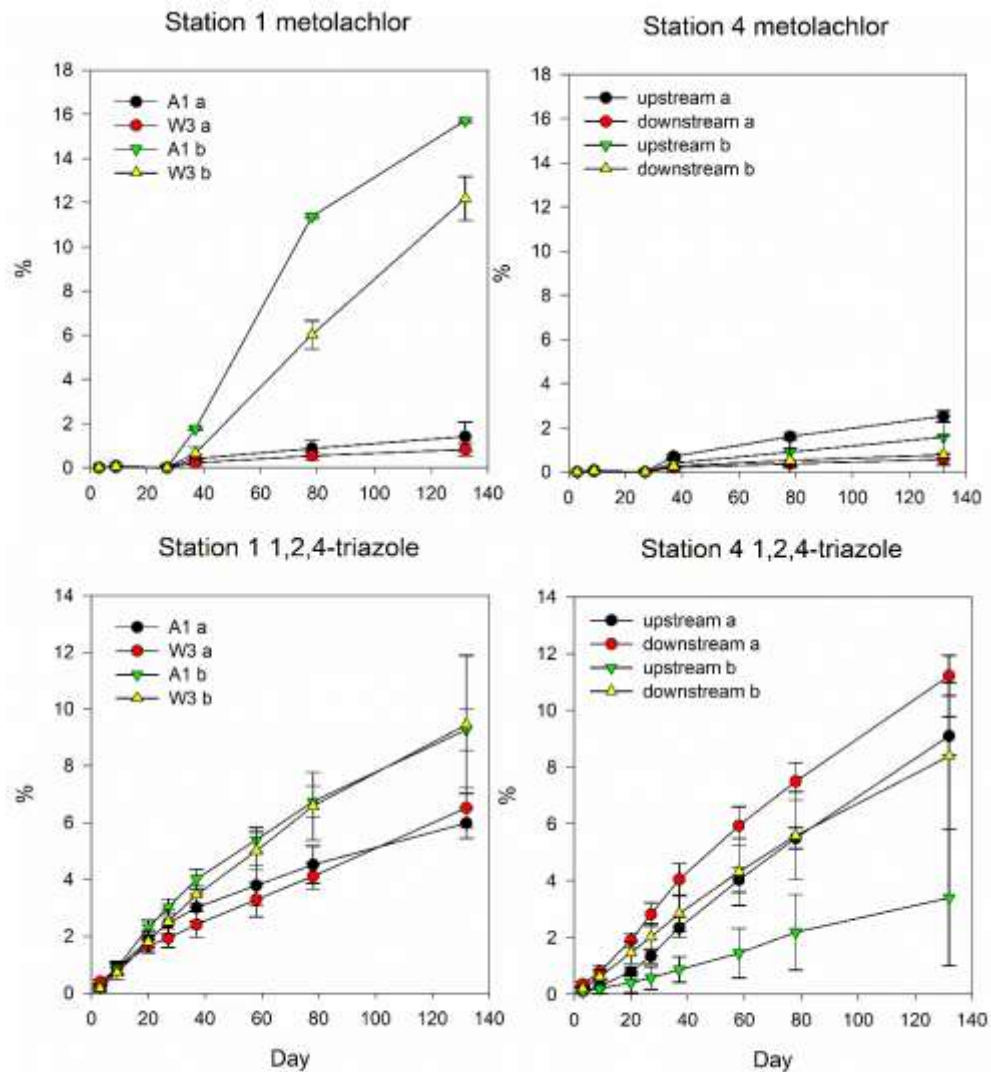


Figure 10. Mineralization of metolachlor and 1,2,4-triazole from sediment at station 1 (left) and station 4 (right). From station 1 A1 is the agricultural side and W3 is the wetland side of the stream. From station 4 there are samples from upstream and downstream. From both stations the a-layer is from ~0-10 cm and the b-layer from ~15-25.

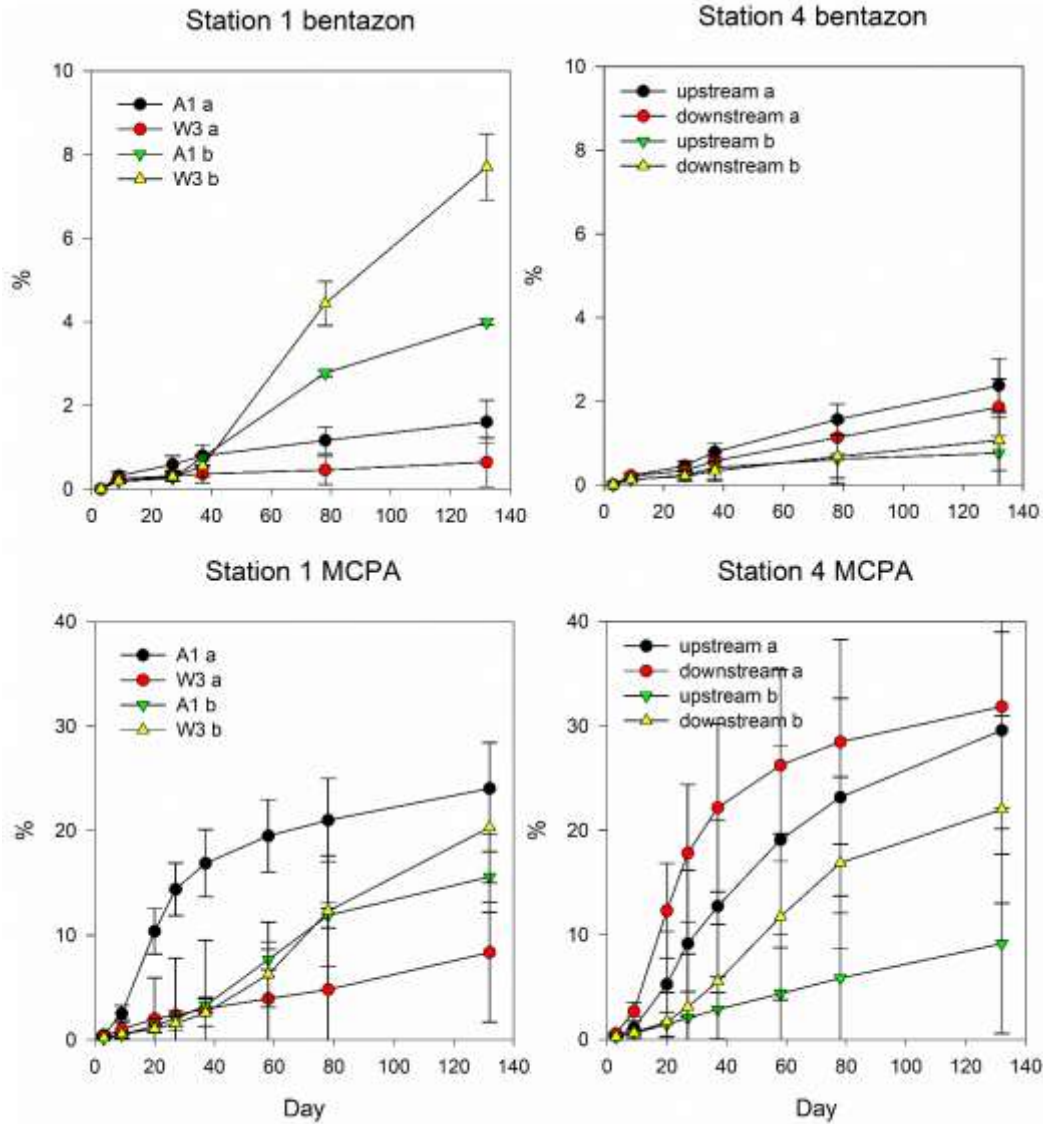


Figure 11. Mineralization of bentazon and MCPA from sediment at station 1 (left) and station 4 (right). From station 1 A1 is the agricultural side and W3 is the wetland side of the stream. From station 4 there are samples from upstream and downstream. From both stations the a-layer is from ~0-10 cm and the b-layer from ~15-25.

Degradation was measured for a total of 16 compounds and transformation products from sulfamethoxazol and metolachlor. In figure 12-14 are presented the data where degradation occurred. Tested compounds that were not degraded included: Propiconazole, chloridazon, metamitron, fenpropimorph, tebuconazole, prothiconazole-desthio, metconazole, epoxiconazole, florasulam, difenoconazole, and bentazon. Estimated  $DT_{50}$  values and times for 50 % removal is presented in table 6 and 7.

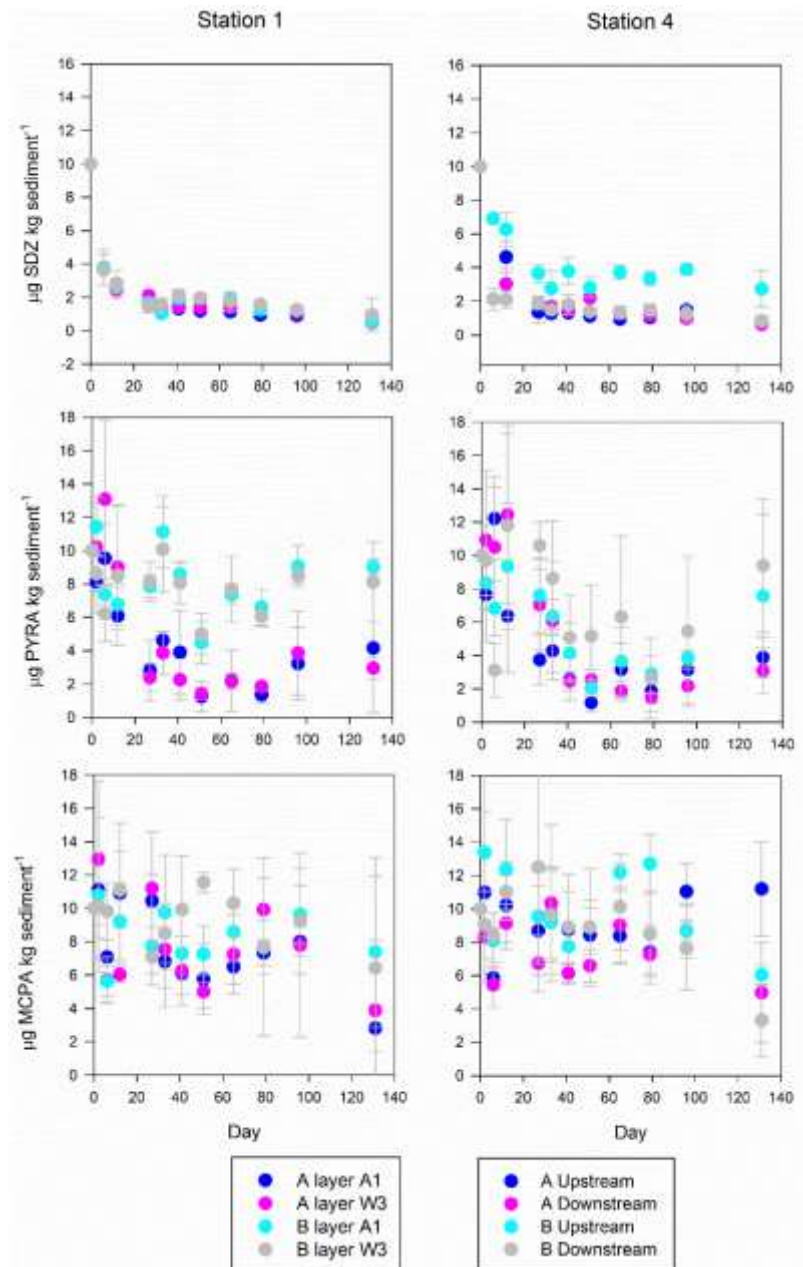


Figure 12. Degradation of Sulfadiazine (SDZ), Pyraclostrobin (PYRA) and MCPA from sediment at station 1 (left) and station 4 (right). Standard deviations are based on four biological replicates (four individual columns) from each depth (A 5-15cm and B 15-25 cm).

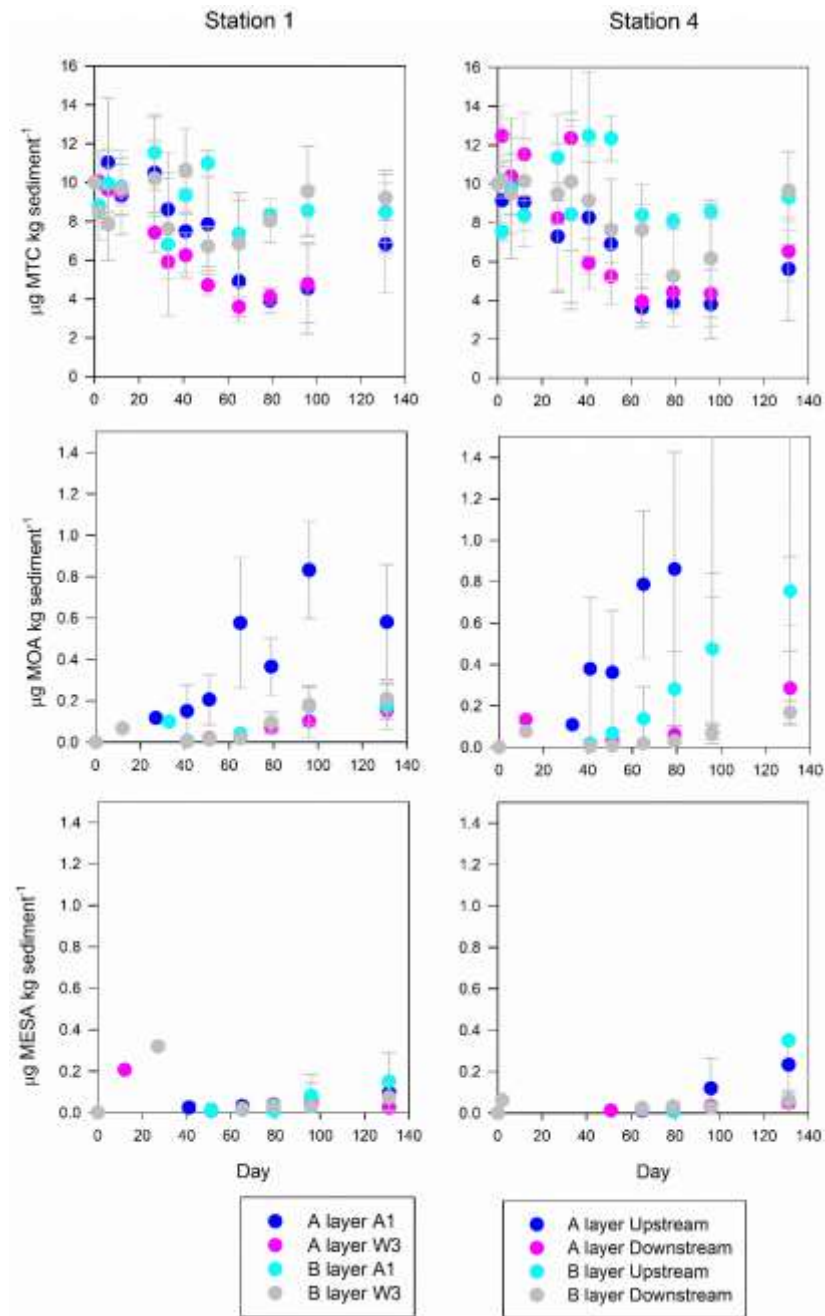


Figure 13. Degradation of metolachlor (upper), and accumulation of MOA (middle) and MESA (lower) from sediments at station 1 (left) and station 4 (right). Standard deviations are based on four biological replicates (four individual columns) from each depth (A 5-15cm and B 15-25 cm).

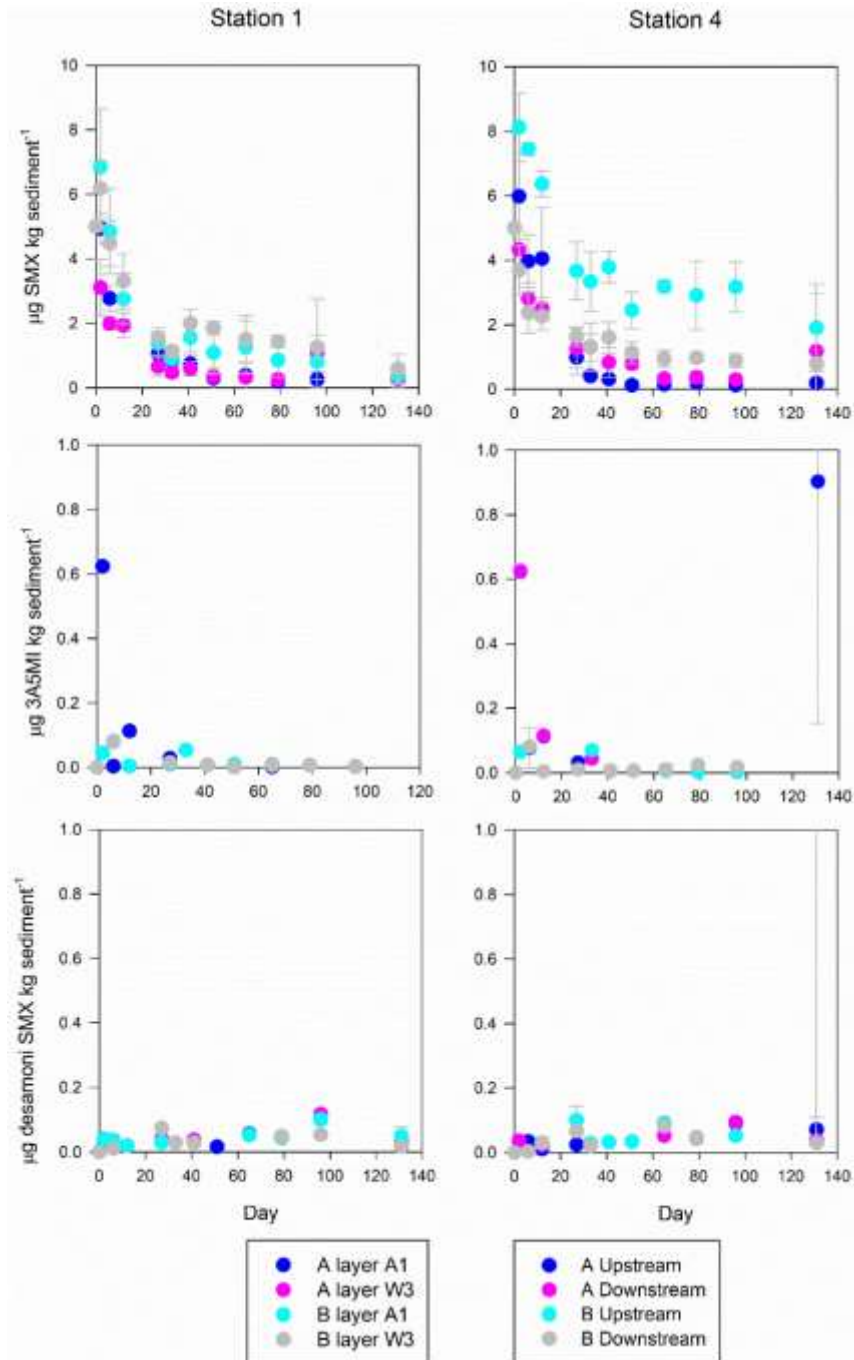


Figure 14. Degradation of sulfamethoxazole (SMX) and development of transformation product 3-amino-5-methylisoxazole (3A5MI) and desamino-SMX in sediments from Holtum stream. Standard deviations are based on four biological replicates (four individual columns) from each depth (A 5-15cm and B 15-25 cm).



## 3.2 Degradation rates (DT<sub>50</sub>)

### 3.2.1 River Crieu

Compared to MCPA mineralization, computed DT<sub>50</sub> values based on degradation were more diverse, ranging from 11 to 44 days, where CP6B and CP7 reveal the slowest degradation. Single-first order kinetics provided the best fit for the degradation of metolachlor and calculated DT<sub>50</sub> values ranged from 2 to 27 (Table 3). For propiconazole single-first order kinetics also provided the best fit for the degradation (Figure 7B), and calculated DT<sub>50</sub> values ranged from 60 to 146 (Table 3).

Table 3. Sediment properties, total organic carbon (TOC), 16S g<sup>-1</sup> sediment, K<sub>d</sub> and DT<sub>50</sub> values for metolachlor, MCPA and propiconazole. Except for TOC all values are based on triplicates.

sediment	TOC	16S	Metolachlor		MCPA		Propiconazole	
	wt %	genes/g sediment	K <sub>d</sub>	DT <sub>50</sub> (d)	K <sub>d</sub>	DT <sub>50</sub> (d)	K <sub>d</sub>	DT <sub>50</sub> (d)
CP3	0,70	6,46E+06	1,58±0,10	22,077	0,23	15,858	7,17±0,73	74,801
CP4	1,26	1,18E+07	2,47±0,41	11,135	0,32	24,013	14,17±3,95	146,478
CP5	1,03	1,27E+07	2,76±0,47	27,411	0,28	11,481	11,33±3,39	94,649
CP6	0,67	9,55E+06	4,20±0,07	1,191	0,24	14,391	19,76±0,66	59,795
CP6B	0,86	1,01E+07	1,79±0,05	5,328	0,13	44,776	8,40±1,01	108,185
CP7	0,19	2,60E+06	7,65±0,19	11,946	0,15	35,152	33,42±1,20	89,764

The Crieu River is often dry in its middle section suggesting water leakage (down-welling) from surface water towards groundwater. On the opposite, the permanent flow observed downstream suggests an input of groundwater into surface water. However, depending on the sampling dates, these phenomena are more or less visible. During the sampling campaign in November 2019, the average river flow rate was 0.39 m<sup>3</sup> s<sup>-1</sup> with no dry sections and its flow decreased from 0.56 to 0.30 m<sup>3</sup> s<sup>-1</sup> between CP4 and CP7, indicating down-welling conditions. Unfortunately, the high flow rate camouflaged downstream changes in the flow rate from the upwelling groundwater which was previously observed.

The degradation rates for metolachlor and propiconazole were in the middle range at CP7 compared to the other calculated DT<sub>50</sub> values. CP7 is characterized by the lowest TOC, lowest 16S gene abundance and upwelling groundwater. A high concentration of organic matter typically increases sorption and thereby decreases bioavailability and therethrough degradation. However, this correlation does not appear to be the dominant factor in these sediments as faster degradation is seen in some of the other sediments with higher TOC levels. Another well known parameter is the biomass, which is the lowest at CP7, again slower degradation is seen in some of the other sediments and may therefore not solely explain the observed data. For MCPA there is a linear correlation between both 16S gene abundance and TOC compared to degradation rates. Furthermore, across the three tested compounds there appears to be the fastest degradation in the CP6 sediment.



### 3.2.2 Risby stream

Measured concentrations are shown in **Erreur ! Source du renvoi introuvable.**9. Single-first order kinetics provided the best fit for most degradation experiments in sediment samples. Degradation of MCPA appeared to be relatively fast with computed  $DT_{50}$  values between 6 and 10 days (**Erreur ! Source du renvoi introuvable.**4) in sediment samples. For metolachlor computed  $DT_{50}$  values were between 18 and 42 days. Propiconazole revealed no degradation during the experiment, and therefore  $DT_{50}$  values have not been calculated.

Table 4. Sediment properties, total organic carbon (TOC), pH,  $16S\ g^{-1}$  sediment,  $K_d$  and  $DT_{50}$  values for metolachlor, MCPA and propiconazole. Except for TOC all values are based on triplicates.

Site	TOC	pH	16S	MCPA		Metolachlor		Propiconazole	
	wt %		gene/g sediment	$DT_{50}$ (d)	$K_d$	$DT_{50}$ (d)	$K_d$	$DT_{50}$ (d)	$K_d$
SM1	2,91	6,78	5,02E+09	9.99	1,32	17,97	12,18	Not degraded	83,03
SM2	3,37	7,01	3,16E+09	6.53		21,78		Not degraded	
SM3	6,23	7,05	2,82E+09	6.09		42,41*		Not degraded	
SM4	3,24	6,76	3,09E+09	8.22		40,90		Not degraded	

\*  $DT_{50}$  value is fitted to the Biexponential-first-order kinetic model (BEFO).

There were no clear differences between sites for sediment degradation experiments that could be linked to TOC, microbial abundance,  $k_d$  or groundwater discharge (SM1 to SM4). Degradation of metolachlor appeared slightly faster at site SM1 and SM2 with a  $DT_{50}$  value of ~20 days compared to values of ~40 days for the other sites (SM3 and SM4). On the contrary, observed degradation of MCPA was slower at site SM1 and SM4 with a  $DT_{50}$  of ~9 days compared to ~6 days for sites SM2 and SM3 (Table 4).

Consequently, a clear influence of groundwater discharge rate on biodegradation potential cannot be concluded from the degradation experiment. In the present setup, SM3 has been impacted the most by pollutants from the landfill, however, SM3 did not differ significantly from the other three sites in regards to its ability to remove the tested pollutants. The inclusion of a bigger set of chemicals could be a possibility to mitigate such shortcomings.

The differences of the included compounds regarding chemical structure, mode of action or environmental fate additionally hamper possible generalizations on the influence of groundwater discharge on biodegradation potentials. Due to these differences amongst the various compounds included in this study, no generalized conclusion on the effect of groundwater discharge on biodegradation potential can be reached. It is likely that other factors, such as pre-exposure to the individual compounds and the coupled adaptation of metabolic capabilities of the bacterial community (Poursat et al., 2019) are responsible for observed differences in biodegradation rates.





### 3.2.3 Holtum stream

Degradation of sulfadiazine, sulfametoxazol, metamitron and pyraclostrobin fitted single-first-order kinetics in all samples (table 5). We observed a general trend of faster degradation in the upper A layer compared to the lower B layer. A similar trend between the two layers were observed for metalochlor and MCPA, when comparing the estimated time for 50 % removal (table 6).

Table 5. Calculated DT<sub>50</sub> (d) values for the compounds that revealed single-first order degradation kinetics.

	Station	Depth	Transect	Sulfadiazine	Sulfametoxazole	Metamitron	Pyraclostrobin
Agriculture	S1	A	A1	13,73	10,78	22,98	21,47
	S1	B	A1	18,40	23,52	42,19	633,72
	S1	A	W3	15,93	9,39	13,03	22,39
	S1	B	W3	20,51	36,51	50,95	320,21
Natural	S4	A	Down stream	14,77	13,83	15,47	22,29
	S4	B	Down stream	43,39	92,75	52,80	32,34
	S4	A	Upstream	20,47	14,81	33,82	28,41
	S4	B	Upstream	16,38	27,27	76,85	45,12

Table 6. Estimated time (d) for 50 % removal (DT<sub>50</sub>) of metalochlor and MCPA, which both were best described by linear regression.

	Station	Depth	Transect	Metolachlor	MCPA
Agriculture	S1	A	A1	107,54	107,46
	S1	B	A1	374,02	466,8
	S1	A	W3	107,19	144,21
	S1	B	W3	1393,88	261,17
Natural	S4	A	Downstream	90,07	slow/no degradation
	S4	B	Downstream	1379,99	272,18
	S4	A	Upstream	96,21	213,26
	S4	B	Upstream	208,49	148,92

When comparing station 1 (agriculture) and station 4 (natural) there is no clear trend that indicates that agriculturally impacted hypoheic sediment have a better degradation potential. Also based on the annual discharge at the 2 sites, where station 4 has 10 times more discharge, this does not seem to solely explain the observed differences in the removal of the tested pollutants. Hence, degradation of different pollutants is most likely influenced by several interacting parameters as described in the introduction covering physical, chemical and hydrological parameters.



## 4 CONCLUSION

The main research interest within WP4 was focused on the influence of flow direction and sorption processes on the biodegradation potential of pesticides and sulfonamides in the hyporheic zone. To address this, we have compared these parameters for the following three sites:

- River Crieu, which was dominated by downwelling conditions in an agriculture dominated catchment.
- Risby River, dominated by upwelling conditions impacted by a landfill
- Holtum River, impacted by upwelling condition in an agricultural dominated catchment

The mineralization and degradation rates/profiles from the sites were different, as highlighted in table 7 which provides an overview of these data. Overall, out of the three study sites, the most compounds were mineralized in the River Crieu sediments covering MCPA, metolachlor, propiconazole (benzen labeled), sulfadiazine, and the degradation product 1,2,4-triazole. Secondly, at the Holtum river MCPA, metalochlor and 1,2,4-triazole were mineralized in some of the sediment samples. Finally, at Risby only MCPA and 1,2,4-triazole were mineralized. For the degradation studies a similar trend was observed between the three sites regarding the number of compounds being degraded.

Table 7 Mineralization and degradation overview of the different compounds. X= mineralization or degradation in ALL sediment samples, (X)= mineralization or degradation in SOME of sediment samples, A = mineralization or degradation in NONE of sediment samples, ND= not detected. TP= Development of transformation products

	River Crieu		Risby River		Holtum River	
	mineralization	degradation	mineralization	degradation	mineralization	degradation
MCPA	X	X	X	X	(X)	(X)
Metolachlor	X	X	A	X	(X)	X
MOA	ND	TP	ND	TP	ND	A
MESA	ND	TP	ND	A	ND	TP
Propiconazole benzen	X	X	A	A	A	A
Propiconazole 1,2,4-triazole	A	X	A	A	A	A
Pyraclostrobin	ND	ND	ND	ND	ND	(X)
Sulfadiazine	X	ND	A	ND	A	A
Sulfametoxazol	ND	X	ND	X	ND	X
3A5	ND	X	ND	A	ND	TP
Desamino-SMX	ND	X	ND	A	ND	TP
Tebuconazole	ND	ND	ND	ND	A	A
1,2,4-triazole	X	ND	X	ND	X	ND
<b>SUM</b>	<b>5X</b>	<b>7X</b>	<b>2X</b>	<b>3X</b>	<b>X + 2 (X)</b>	<b>2X + (X)</b>

As discussed in the result section there is no clear trend between sorption properties and the degradation potential or to the TOC level as often seen in the literature. This indicates that the



---

processes governing the degradation of organic pollutants in hypoxic sediments are quite complex and has to include several interrelated parameters including chemical, physical and biological factors at the same time.

Based on the three sites presented in this deliverable, it is not possible to make a solid conclusion on the influence of upwelling and downwelling conditions. However, our data reveal that the largest number of degraded organic pollutants occurs at the River Crieu, which coincides with the downwelling conditions.

The influence of bacterial abundance and diversity is a known factor influencing the degradation potential. This will be presented and discussed further in deliverable D4.3.



## 5 REFERENCES

- Amalric, L., Baran, N., Coureau, C., Maingot, L., Buron, F., Routier, S., 2013. Analytical developments for 47 pesticides: first identification of neutral chloroacetanilide derivatives in French groundwater. *Int. J. Environ. Anal. Chem.* 93, 1660–1675. <https://doi.org/10.1080/03067319.2013.853758>
- Aubeneau, A.F., Drummond, J.D., Schumer, R., Bolster, D., Tank, J.L., Packman, A.I., 2015. Effects of benthic and hyporheic reactive transport on breakthrough curves. <https://doi.org/10.1086/680037> 34, 301–315. <https://doi.org/10.1086/680037>
- Bælum, J., Prestat, E., David, M.M., Strobel, B.W., Jacobsen, C.S., 2012. Modeling of phenoxy acid herbicide mineralization and growth of microbial degraders in 15 soils monitored by quantitative real-time PCR of the functional *tfdA* gene. *Appl. Environ. Microbiol.* 78, 5305–5312. <https://doi.org/10.1128/AEM.00990-12>
- Batioğlu-Pazarbaşı, M., Milosevic, N., Malaguerra, F., Binning, P.J., Albrechtsen, H.-J., Bjerg, P.L., Aamand, J., 2013. Discharge of landfill leachate to streambed sediments impacts the mineralization potential of phenoxy acid herbicides depending on the initial abundance of *tfdA* gene classes. *Environ. Pollut.* 176, 275–283. <https://doi.org/10.1016/J.ENVPOL.2013.01.050>
- Battin, T.J., Besemer, K., Bengtsson, M.M., Romani, A.M., Packmann, A.I., 2016. The ecology and biogeochemistry of stream biofilms. *Nat. Rev. Microbiol.* 2016 144 14, 251–263. <https://doi.org/10.1038/nrmicro.2016.15>
- Boano, F., Harvey, J.W., Marion, A., Packman, A.I., Revelli, R., Ridolfi, L., Wörman, A., 2014. Hyporheic flow and transport processes: Mechanisms, models, and biogeochemical implications. *Rev. Geophys.* 52, 603–679. <https://doi.org/10.1002/2012RG000417>
- Harvey, J.W., Böhlke, J.K., Voytek, M.A., Scott, D., Tobias, C.R., 2013. Hyporheic zone denitrification: Controls on effective reaction depth and contribution to whole-stream mass balance. *Water Resour. Res.* 49, 6298–6316. <https://doi.org/10.1002/WRCR.20492>
- Hebig, K.H., Groza, L.G., Sabourin, M.J., Scheytt, T.J., Ptacek, C.J., 2017. Transport behavior of the pharmaceutical compounds carbamazepine, sulfamethoxazole, gemfibrozil, ibuprofen, and naproxen, and the lifestyle drug caffeine, in saturated laboratory columns. *Sci. Total Environ.* 590–591, 708–719. <https://doi.org/10.1016/J.SCITOTENV.2017.03.031>
- Houmark-Nielsen, M., 1989. The last interglacial-glacial cycle in Denmark. *Quat. Int.* 3–4, 31–39. [https://doi.org/10.1016/1040-6182\(89\)90071-2](https://doi.org/10.1016/1040-6182(89)90071-2)
- Köhler, H.R., Triebkorn, R., 2013. Wildlife ecotoxicology of pesticides: Can we track effects to the population level and beyond? *Science* (80-. ). 341, 759–765. <https://doi.org/10.1126/SCIENCE.1237591>
- Krause, S., Heathwaite, L., Binley, A., Keenan, P., 2009. Nitrate concentration changes at the groundwater-surface water interface of a small Cumbrian river, in: *Hydrological Processes*. John Wiley & Sons, Ltd, pp. 2195–2211. <https://doi.org/10.1002/hyp.7213>
- Lewandowski, J., Arnon, S., Banks, E., Batelaan, O., Betterle, A., Broecker, T., Coll, C., Drummond, J.D., Garcia, J.G., Galloway, J., Gomez-Velez, J., Grabowski, R.C., Herzog, S.P., Hinkelmann, R., Höhne, A., Hollender, J., Horn, M.A., Jaeger, A., Krause, S., Prats, A.L., Magliozzi, C., Meinikmann, K., Mojarrad, B.B., Mueller, B.M., Peralta-Maraver, I., Popp, A.L., Posselt, M., Putschew, A., Radke, M., Raza, M., Riml, J., Robertson, A., Rutere, C., Schaper, J.L., Schirmer, M., Schulz, H., Shanafield, M., Singh, T., Ward, A.S., Wolke, P., Wörman, A., Wu, L., 2019. Is the Hyporheic Zone Relevant beyond the Scientific Community? *Water* 2019, Vol. 11, Page 2230 11, 2230. <https://doi.org/10.3390/W11112230>



- Lewandowski, J., Putschew, A., Schwesig, D., Neumann, C., Radke, M., 2011. Fate of organic micropollutants in the hyporheic zone of a eutrophic lowland stream: Results of a preliminary field study. *Sci. Total Environ.* 409, 1824–1835. <https://doi.org/10.1016/j.scitotenv.2011.01.028>
- Munz, M., Oswald, S.E., Schäfferling, R., Lensing, H.J., 2019. Temperature-dependent redox zonation, nitrate removal and attenuation of organic micropollutants during bank filtration. *Water Res.* 162, 225–235. <https://doi.org/10.1016/J.WATRES.2019.06.041>
- Peralta-Maraver, I., Reiss, J., Robertson, A.L., 2018. Interplay of hydrology, community ecology and pollutant attenuation in the hyporheic zone. *Sci. Total Environ.* <https://doi.org/10.1016/j.scitotenv.2017.08.036>
- Posselt, M., Mechelke, J., Rutere, C., Coll, C., Jaeger, A., Raza, M., Meinikmann, K., Krause, S., Sobek, A., Lewandowski, J., Horn, M.A., Hollender, J., Benskin, J.P., 2020. Bacterial Diversity Controls Transformation of Wastewater-Derived Organic Contaminants in River-Simulating Flumes. *Environ. Sci. Technol.* 54, 5467–5479. <https://doi.org/10.1021/acs.est.9b06928>
- Poulsen, J.R., Sebok, E., Duque, C., Tetzlaff, D., Engesgaard, P.K., 2015. Detecting groundwater discharge dynamics from point-to-catchment scale in a lowland stream: Combining hydraulic and tracer methods. *Hydrol. Earth Syst. Sci.* 19, 1871–1886. <https://doi.org/10.5194/HESS-19-1871-2015>
- Poursat, B.A.J., Spanning, R.J.M. van, Voogt, P. de, Parsons, J.R., 2019. Implications of microbial adaptation for the assessment of environmental persistence of chemicals. *Environ. Sci. Technol.* 49, 2220–2255. <https://doi.org/10.1080/10643389.2019.1607687>
- Rutherford, J.E., Hynes, H.B.N., 1987. Dissolved organic carbon in streams and groundwater. *Hydrobiologia* 154, 33–48. <https://doi.org/10.1007/BF00026829>
- Smith, J.W.N., 2005. Groundwater – surface water interactions in the hyporheic zone, Environment Agency Science report SC030155/SR1, Environment Agency: Bristol, UK.
- Stegen, J.C., Fredrickson, J.K., Wilkins, M.J., Konopka, A.E., Nelson, W.C., Arntzen, E. V., Chrisler, W.B., Chu, R.K., Danczak, R.E., Fansler, S.J., Kennedy, D.W., Resch, C.T., Tfaily, M., 2016. Groundwater–surface water mixing shifts ecological assembly processes and stimulates organic carbon turnover. *Nat. Commun.* 2016 71 7, 1–12. <https://doi.org/10.1038/ncomms11237>
- White, J., 1990. The use of sediment traps in high-energy environments. *Mar. Geophys. Res.* 12, 145–152. <https://doi.org/10.1007/BF00310569>
- Wondzell, S.M., 2011. The role of the hyporheic zone across stream networks. *Hydrol. Process.* 25, 3525–3532. <https://doi.org/10.1002/hyp.8119>